Available online at www.sciencedirect.com
ScienceDirect
Journal of Catalysis 244 (2006) 17–23
JOURNAL OF CATALYSIS
www.elsevier.com/locate/jcat

Effect of ZnO additives and acid treatment on catalytic performance of $Pt/WO_3/ZrO_2$ for n-C_7 hydroisomerization

Yan Liu [a,*], Yejun Guan [b], Can Li [b], Juan Lian [a], Geok Joo Gan [a], Eng Chew Lim [a], Fethi Kooli [a]

[a] *Institute of Chemical and Engineering Sciences, 1 Pesek Road, Jurong Island, Singapore 627833*
[b] *State Key Laboratory of Catalysis, Dalian Institute of Chemical Physics, Dalian 116023, China*

Received 16 August 2006; revised 18 August 2006; accepted 19 August 2006

Available online 26 September 2006

Abstract

The effect of WO_3 (5–50 wt%) and ZnO (0.7–22 wt%) on the catalytic properties of $Pt/WO_3/(ZnO)–ZrO_2$ for n-heptane (n-C_7) hydroisomerization was investigated. The optimized WO_3 and ZnO contents are 20 wt% and 3.4 wt%, respectively. The catalytic performance is achieved at 81% n-C_7 conversion and 89% C_7 isomer selectivity at 250 °C, which is reproducible and can be kept constant over 82 h under reaction conditions. Both WO_3 and ZnO can stabilize the tetragonal phase of ZrO_2. The Brønsted acid-to-Lewis acid ratio should be optimized to achieve high catalytic performance. The activity for $Pt/WO_3/ZrO_2$ using $Zr(OH)_4$ as the catalyst support (n-C_7 conversion, 88% at 250 °C) is much higher than that for $Pt/WO_3/ZrO_2$ with ZrO_2 as the support (n-C_7 conversion, 9% at 250 °C) with the same Pt and WO_3 loadings. BET, SEM-EDX, and pyridine-FTIR analyses show that acid treatment can successfully enhance the surface area (from 73 to 91 m^2/g), increase the number of Brønsted acid sites, and lower the surface Zn:Zr ratio (from 0.43 to 0.15) for $ZnO–ZrO_2$ with 22 wt% ZnO. The yield of C_7 isomers is increased from nil to 47% at 300 °C on $Pt/WO_3/ZnO–ZrO_2$ catalyst after acid treatment. It is suggested that n-heptane hydroisomerization activity is related to acidity, surface area, and crystalline phase of ZrO_2.

Keywords: $Pt/WO_3–ZrO_2$ catalysts; ZnO; Acid treatment; n-Heptane hydroisomerization; Pyridine-FTIR

1. Introduction

Environmentally driven regulations are requiring significant improvement in the quality of diesel and gasoline in many parts of the world [1]. Reducing the concentrations of aromatic compounds has been recognized as one way to meet the requirement of "clean fuels" [2], which may be accompanied by a drop in octane number. One potential solution is to isomerize the straight-chain paraffins with low octane number, which are a major constituent in some crude oil fraction, into the branched isomers with high octane number as octane-enhancing components. Consequently, the isomerization of C_{7+} has reemerged as the researchers' interest and is becoming increasingly popular from both scientific and industrial standpoints [3–6].

Unlike C_4–C_6 isomerization, alkane conversion above C_7 to their multibranched components in the selective alkane isomerization is rather difficult. This is attributed to the ease of cracking by β-scission. These components have large numbers of methylene species that, in the presence of Lewis acids, can form carbenium ions by abstraction of hydride ions [7] or, in strong Brønsted acids, can form carbonium ions [8]. It is highly desirable to obtain environmentally clean catalysts that can be used to isomerize long-chain paraffins with minimum cracking.

Recently, metal oxides promoted by sulfur compounds were studied as strong solid acid catalysts, particularly SO_4^{2-}-promoted zirconia containing noble metal to inhibit catalyst deactivation [9]. However, the low isomerization selectivity for C_{7+} alkanes, poor stability, and tendency to form volatile sulfur compounds during catalysis and regeneration limit their further applicability.

Tungsten-related solid acids, especially $Pt/WO_3–ZrO_2$, with mild acidity, show good activity and selectivity for alkane isomerization and have been investigated in n-heptane isomer-

* Corresponding author. Fax: +65 63166182.
E-mail address: liu_yan@ices.a-star.edu.sg (Y. Liu).

0021-9517/$ – see front matter
doi:10.1016/j.jcat.2006.08.015

ization [10–16]. Iglesia et al. showed that $Pt/SO_4^{2-}/ZrO_2$ and $Pt/WO_x/ZrO_2$ exhibited similar activity for low-temperature (200 °C) *n*-heptane isomerization, but $Pt/WO_x/ZrO_2$ was significantly more active at high reaction temperature (250 °C) [17]. This was attributed to the greater stability of $Pt/WO_x/ZrO_2$ to deactivation by sublimation or decomposition of the acid sites at higher reaction temperatures. These authors also observed that $Pt/WO_x/ZrO_2$ has much higher isomerization selectivity than $Pt/SO_4^{2-}/ZrO_2$. This was attributed to the loss of a hydrogen activating metal function due to sulfur poisoning of the Pt particles in $Pt/SO_4^{2-}/ZrO_2$ [18].

The isomerization reaction is a bifunctional catalytic process [19]. The balance between the hydrogenation–dehydrogenation function and acidity is crucial for determining activity, stability, and product selectivity [20,21]. In the present study, ZnO base additives and acid treatment method were varied to adjust the acidity of the catalysts. The resulting catalysts, $Pt/WO_3/(ZnO)–ZrO_2$, was investigated for n-C_7 hydroisomerization. We found that an appreciable amount of ZnO can stabilize the tetragonal phase of ZrO_2 and affect acidity, and that acid treatment can remove extra ZnO on the surface and further enhance catalytic performance.

2. Experimental

2.1. Catalysts

$Zr(OH)_4$ and $Zn(OH)_2$–$Zr(OH)_4$ materials were prepared using a precipitation method. Briefly, an alkaline slurry (pH 10) containing $ZrOCl_2$ (with or without $ZnCl_2$) and ammonium hydroxide was heated to 90 °C for 4 h. The product was filtered, washed with excess water until it was Cl^- free, and then dried overnight at 110 °C. ZrO_2 and ZnO–ZrO_2 were obtained by calcination at appropriate temperature and time.

ZnO–ZrO_2 with 22 wt% ZnO loading calcined at 500 °C was treated in dilute HCl solution (0.3 M) at room temperature for 4 h. Then the powder was filtered, washed with excess water, and dried overnight at 110 °C.

WO_3 was introduced by impregnation with a precalculated amount of $(NH_4)_6W_{12}O_{39}$ solution overnight, then dried at 110 °C for 24 h, followed by calcination at 800 °C for 3 h. $Zn(OH)_2$–$Zr(OH)_4$, $Zr(OH)_4$, ZrO_2, and ZnO–ZrO_2 before and after acid treatment were used as the supports unless indicated otherwise. H_4PtCl_6 solution was used for Pt impregnation on $WO_3/(ZnO)–ZrO_2$. Then the impregnated sample was dried at 110 °C for 24 h, followed by calcination at 500 °C for 3 h.

2.2. Catalyst characterization

Powder X-ray diffraction (XRD) data were collected using Cu$K\alpha$ radiation on a Bruker D8 Advance diffractometer. An automated adsorption apparatus (Autosorb-6B, Quantachrome) was used for specific surface area and pore size distribution analysis. XPS analysis was carried out using an ESCALAB 250 spectroscope (Thermo VG Scientific). FTIR experiments were investigated on a Thermo Nicolet NEXUS 470 FTIR spectrometer with 64 scans at 4 cm^{-1} resolution. All samples were pressed into self-supporting wafers and treated at 400 °C for 1 h in vacuo or in H_2 gas (flow rate, 80 cm^3/min) in a quartz IR cell. Once the samples were cooled to room temperature, a background was recorded. After being exposed to pyridine vapor at ambient temperature for 10 min, the wafers were outgassed at 150 °C for 1 h, and then IR spectra were collected at room temperature. All spectra were differences between the spectra of samples with adsorbed pyridine and the backgrounds.

2.3. Catalytic test conditions

Catalytic activity analysis was carried out at atmospheric pressure in a tubular quartz glass, fixed-bed reactor. Each run used approximately 300 mg of catalyst in the form of 30–80 mesh particles. Before catalytic measurements, the catalysts were reduced at 400 °C using H_2 (30 ml/min) for 2 h. *n*-Heptane was introduced to the reactor by a carrier gas of H_2 flowing through a saturator maintained at 16 °C. The flow rate was 30 ml/min. Catalytic tests were performed at a temperature range of 250–350 °C, measured using a thermocouple projecting into the catalyst bed. The product gas mixture was analyzed periodically (one analysis every 22 min) on-line with a HP 6890N gas chromatograph equipped with a flame ionization detector and a HP-PONA (50 m × 0.2 mm) capillary column.

3. Results and discussion

3.1. XRD analysis

Fig. 1 displays the XRD analysis of the calcined WO_3/ZrO_2 mixture with different WO_3 loadings at 800 °C. The intensity of the monoclinic phase of ZrO_2 decreased gradually with the amount of WO_3 loading, indicating that WO_3 can stabilize the tetragonal phase of ZrO_2, in agreement with previous reports

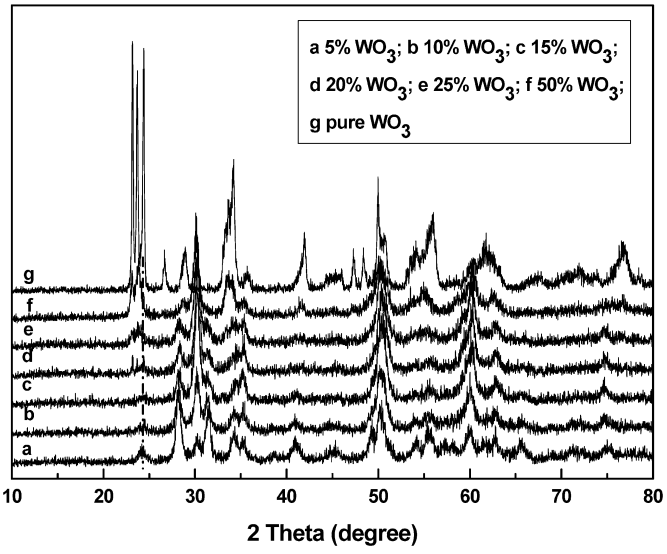

Fig. 1. XRD patterns of WO_3/ZrO_2 with different WO_3 loadings calcined at 800 °C (2θ at 30.3°, 35.4°, 50.2°, and 60° are assigned to tetragonal phase, while 2θ at 24°, 28.3°, 31.5°, 34.3°, 36.4°, 41°, 49.4°, 54.1°, 55.4°, and 65.7° are due to monoclinic phase of ZrO_2).

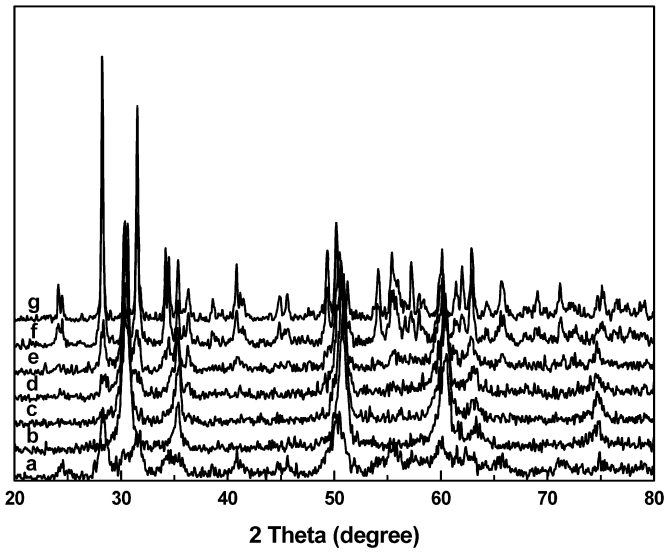

Fig. 2. XRD patterns of ZrO_2 calcined at 500 °C (a), ZnO–ZrO_2 (with 22 wt% ZnO) calcined at 500 (b), 600 (c), 650 (d), 700 (e), 800 (f), and 900 °C (g).

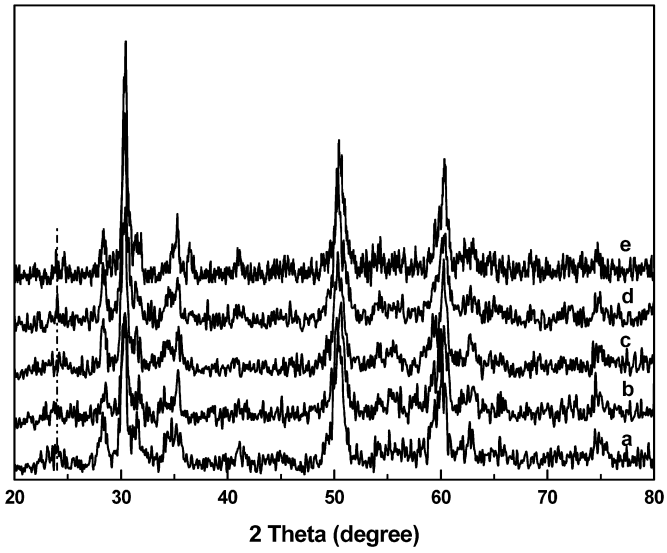

Fig. 3. XRD patterns of WO_3/ZnO–ZrO_2 (WO_3: 20 wt%) calcined at 800 °C with different ZnO contents: (a) 0, (b) 0.7, (c) 3.4, (d) 6.8, and (e) 22 wt%.

[22–24]. When WO_3 content exceeds 25 wt%, the XRD pattern shows the presence of WO_3 crystalline phase.

As an additive, ZnO-modified ZnO–ZrO_2 was calcined at different temperatures and characterized by XRD. As shown in Fig. 2, ZrO_2 with 500 °C calcination was a mixture of tetragonal and monoclinic phases, with monoclinic the primary phase. However, when 22 wt% of ZnO was introduced, at the same calcination temperature (500 °C), ZnO–ZrO_2 exhibited the pure tetragonal phase of ZrO_2, which can be maintained up to 650 °C. This suggests that ZnO can also stabilize the tetragonal phase of ZrO_2. At calcination temperatures above 650 °C, ZnO–ZrO_2 showed a mixture of tetragonal and monoclinic phases of ZrO_2.

Further XRD studies on Pt/WO_3/ZnO–ZrO_2 with varying ZnO content suggested that ZnO can stabilize the tetragonal phase of ZrO_2, as shown in Fig. 3. The XRD peaks representing the monoclinic phase of ZrO_2 decreased with increasing ZnO contents.

3.2. Catalytic activity of Pt/WO_3/ZrO_2 with different WO_3 loadings

Pt/WO_3/ZrO_2 with different WO_3 loadings was investigated for *n*-heptane isomerization in a fixed-bed reactor under atmospheric pressure. Pure ZrO_2, WO_3, and Pt/ZrO_2 showed no activity at 250 °C. When WO_3 was introduced to Pt/ZrO_2, conversion and C_7 isomer selectivity improved significantly (Fig. 4). The highest conversion of *n*-heptane (88%) was achieved with a 20-wt% WO_3 addition. Meanwhile, the highest selectivity of 90% was obtained with a 15 wt% loading of WO_3. (Ignore the selectivity for the catalyst with 5 wt% WO_3, because the conversion is too low at 0.1%.) The yields for the catalysts with 15 and 20 wt% WO_3 loadings did not differ significantly (58 vs 57%). Thus, unless indicated otherwise, the WO_3 and Pt loadings were fixed at 20 wt% and 0.5 wt% for subsequent studies. Further addition of WO_3 led to a decrease in both conversion (to 18%) and C_7 isomer yield (to 15%) for the catalyst with 50 wt% WO_3 loading. BET analysis (Fig. 5) indicated that the surface area of Pt/WO_3/ZrO_2 (25 wt%) was still comparable to those of catalysts with lower WO_3 loadings. However, when WO_3 loading reached 50 wt%, surface area decreased significantly. Correlating these findings with the XRD analysis results discussed in Section 3.1 suggests that the isomerization reaction is catalyzed by certain W atoms working synergistically [11]. Too much W (crystalline WO_3) will have a negative effect on the *n*-C_7 hydroisomerization reaction as well as on the surface area. Cortés-Jácome et al. reported that WO_x species distributed homogeneously on the surface of the tetragonal ZrO_2 are the active species participating in the reaction [11,12], and that well-crystallized WO_3 phase with large particles is less active for *n*-hexane isomerization [24].

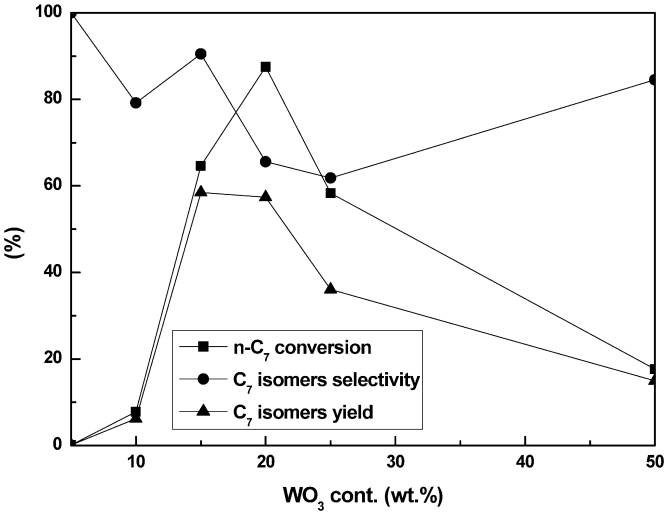

Fig. 4. Catalytic activity of *n*-C_7 hydroisomerization on Pt/WO_3/ZrO_2 with different WO_3 loadings (catalyst: 300 mg; Pt: 0.5 wt%; reduction: H_2, 30 ml/min, 400 °C, 2 h; reaction: 250 °C, 0.1 MPa, H_2/*n*-C_7 = 30:1).

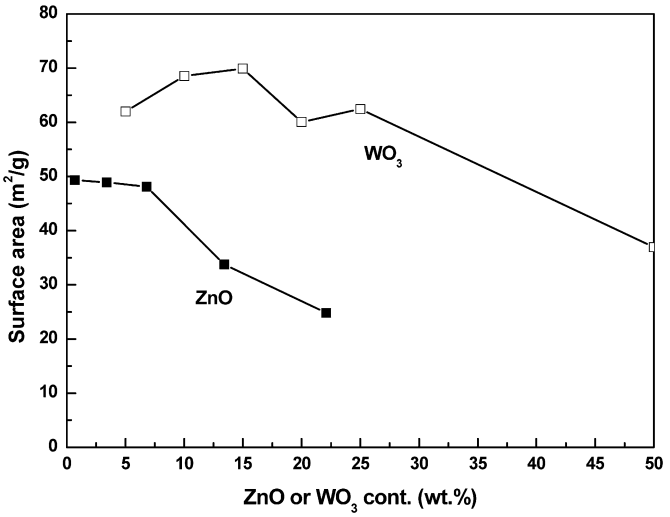

Fig. 5. BET analysis for $Pt/WO_3/ZrO_2$ with different WO_3 contents (Pt: 0.5 wt%) and $Pt/WO_3/ZnO–ZrO_2$ with different ZnO contents (Pt: 0.5 wt%; WO_3: 20 wt%).

3.3. Catalytic activity of $Pt/WO_3/ZnO–ZrO_2$ with different ZnO loadings

Fig. 6 displays n-C_7 conversion, selectivity, and yield of C_7 isomers versus ZnO loading at 250 °C. Adding ZnO enhanced both the selectivity and the yield of C_7 isomers. The yield reached a maximum of 72% with 3.4 wt% of ZnO loading, compared with the 57% C_7 isomer yield for ZnO-free catalyst. However, further addition of ZnO up to 6.8 wt% led to a decreased C_7 isomer yield of 39%. The ZnO content at 6.8 wt% is also a critical determinant of surface area, as shown in Fig. 5. No activity was achieved for a high ZnO loading of 22 wt%, which also led to a quite low surface area. As reported, only a specific optimal balance of metal and acid function at suitable reaction conditions can suppress cracking to achieve high isomerization selectivity for long-chain alkanes [25,26]. At reaction temperatures as low as 200 °C, both $Pt/WO_3/ZrO_2$ and $Pt/WO_3/ZnO–ZrO_2$ with ZnO loadings of 0.7–13.6 wt% gave low n-C_7 conversion with quite high C_7 isomer selectivity and a trace amount of cyclo products, which are all clean blender for gasoline production.

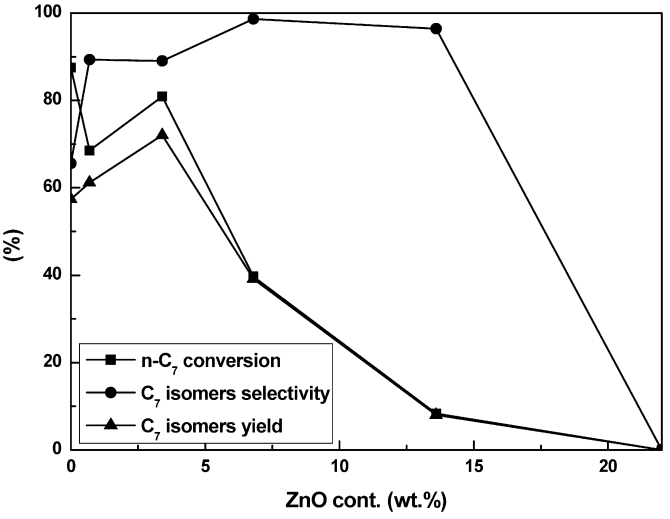

Fig. 6. Catalytic activity of n-C_7 hydroisomerization on $Pt/WO_3/ZnO–ZrO_2$ with different ZnO loadings (catalyst: 300 mg; Pt: 0.5 wt%; WO_3: 20 wt%; reduction: H_2, 30 ml/min, 400 °C, 2 h; reaction: 250 °C, 0.1 MPa, H_2/n-C_7 = 30:1).

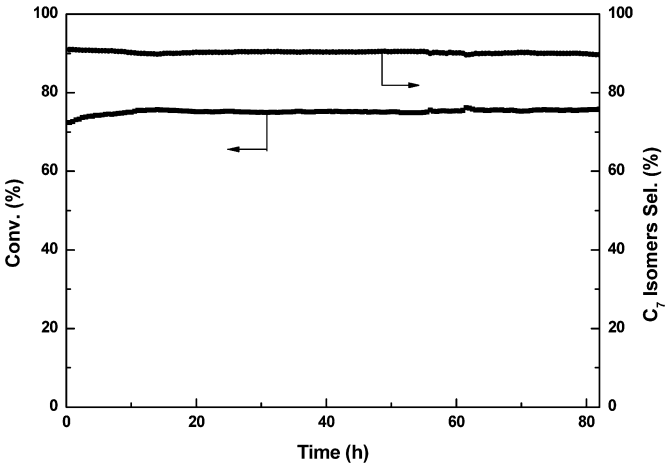

Fig. 7. n-Heptane hydroisomerization activity of $Pt/WO_3/ZnO–ZrO_2$ with 3.4 wt% ZnO loading (catalyst: 300 mg; Pt: 0.5 wt%; WO_3: 20 wt%; reduction: H_2, 30 ml/min, 400 °C, 2 h; reaction: 250 °C, 0.1 MPa, H_2/n-C_7 = 30:1).

After reaction, $Pt/WO_3/ZnO–ZrO_2$ catalysts with different ZnO loadings were characterized by XPS. The results indicate that all of the catalysts investigated here gave the same banding energy for either Pt (71.32 and 74.35 eV) or W (37.76 and 35.68 eV) (data not shown), suggesting that ZnO loading did not affect the reducibility of Pt and WO_3 during either reduction activation or the reaction process for n-C_7 hydroisomerization.

The stability of a specific catalyst is an important issue in catalyst design. Long-reaction activity was tested for $Pt/WO_3/ZnO–ZrO_2$ with a 3.4 wt% ZnO loading. As shown in Fig. 7, n-C_7 conversion remained stable at 81% for at least 82 h at 250 °C, with selectivity to C_7 isomers of around 89%. Reproducibility testing for $Pt/WO_3/ZnO–ZrO_2$ catalyst with a 3.4 wt% ZnO loading was also carried out; as shown in Fig. 8, the activity data for the reprepared catalysts are quite reproducible to the former.

3.4. Acidity characterization for $Pt/WO_3/ZnO–ZrO_2$ with different ZnO loadings

Acidity was characterized by in situ FTIR using pyridine as a probe molecule [27,28]. Fig. 9 shows the FTIR spectra of pyridine desorbed at 150 °C in the range of 1700–1400 cm^{-1} for catalysts with different ZnO loadings. The bands related to pyridine adsorbed on Lewis acid sites were recorded at 1451 and 1611 cm^{-1}, whereas the pyridine adsorbed on the Brønsted acid sites was detected at 1536 and 1640 cm^{-1}, respectively. The band at 1490 cm^{-1} was attributed to pyridine associated with both Lewis and Brønsted acid sites [29,30]. The acid properties of the catalyst are presented using the Brønsted acid-to-Lewis acid ratio from their specific bands, namely an IR band at 1536 cm^{-1} for Brønsted acid and an IR band at 1611 cm^{-1} for Lewis acid. These values were 0.85, 0.72, 0.69, and 0.43 for

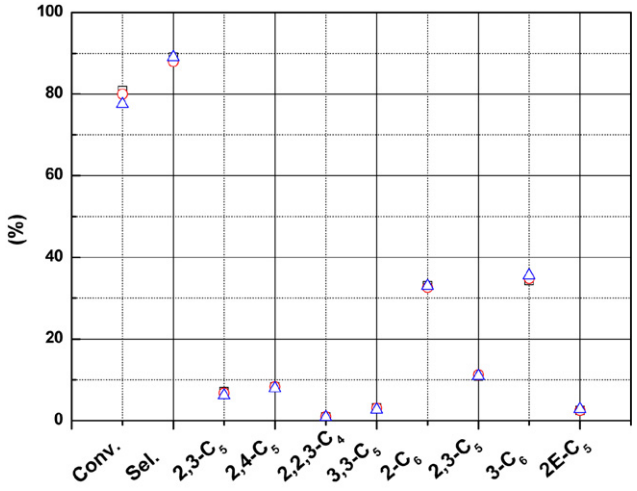

Fig. 8. The reproducibility investigation for conversion, selectivity and products distribution for C_7 isomers for $Pt/WO_3/ZnO–ZrO_2$ (catalyst: 300 mg; Pt: 0.5 wt%; WO_3: 20 wt%; ZnO: 3.4 wt%; reduction: H_2, 30 ml/min, 400 °C, 2 h; reaction: 250 °C, 0.1 MPa, H_2/n-$C_7 = 30:1$; 2,3-C_5: 2,3-dimethyl-pentane; 2,4-C_5: 2,4-dimethyl-pentane; 2,2,3-C_4: 2,2,3-trimethyl-butane; 3,3-C_5: 3,3-dimethyl-pentane; 2-C_6: 2-methyl-hexane; 2,3-C_5: 2,3-dimethyl-pentane; 3-C_6: 3-methyl-hexane; 2E-C_5: 2-ethyl-pentane).

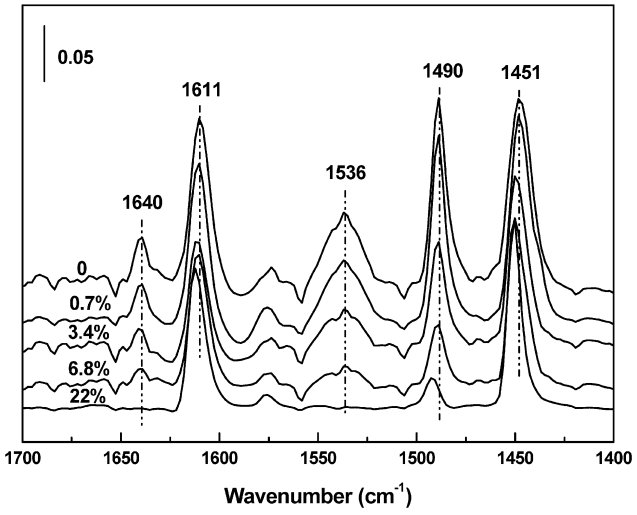

Fig. 9. Pyridine-FTIR characterizations of $Pt/WO_3/ZrO_2$ with different ZnO loadings.

$Pt/WO_3/ZrO_2$ and $Pt/WO_3/ZnO–ZrO_2$ with 0.7 wt%, 3.4 wt%, and 6.8 wt% ZnO loadings, respectively. When the ZnO loading reached 22 wt%, pyridine-FTIR analysis detected no Brønsted acid sites. As shown in Fig. 6, the highest yield of C_7 isomers was achieved for the catalyst with 3.4 wt% ZnO loading, and C_7 isomer yield decreased when ZnO loading was $\geqslant$6.8 wt%. This finding suggests that the n-C_7 hydroisomerization requires a specific ratio of Brønsted acid sites to Lewis acid sites on the catalyst surface.

3.5. Effects of impregnation procedures for $Pt/WO_3/ZrO_2$

The effect of the impregnation procedure was also investigated. Table 1 presents catalytic data for the two catalysts prepared with different support precursors. Higher conversion

Table 1
Effects from impregnation procedures for $Pt/WO_3–ZrO_2$

Solids for impregnation	T (°C)	Conversion (%)	Selectivity (%)	Isomer distribution		
				MB	DB	TB
$Zr(OH)_4$	250	88	66	66	32	1
	300	99	4	56	40	4
	350	100	0	0	0	0
ZrO_2	250	9	87	100	0	0
	300	68	76	78	22	0.4
	350	95	25	66	32	2

Catalyst: 300 mg; Pt: 0.5 wt%; WO_3: 20 wt%; reduction: H_2, 30 ml/min, 400 °C, 2 h; reaction: 250 °C, 300 °C, 350 °C, 0.1 MPa, H_2/n-$C_7 = 30:1$; MB: monobranched C_7 isomers; DB: dibranched C_7 isomers; TB: tribranched C_7 isomers.

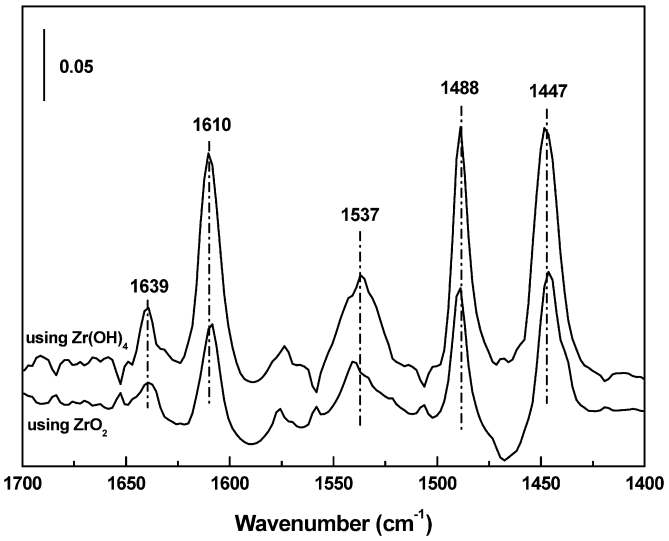

Fig. 10. Pyridine-FTIR characterizations for $Pt/WO_3/ZrO_2$ using either $Zr(OH)_4$ or ZrO_2 for impregnation.

was achieved when $Zr(OH)_4$ was used as a starting support precursor for catalyst preparation (by impregnation of W and Pt), compared with that achieved when using ZrO_2 as a starting support, as reported previously [31]. At 250 °C, the n-C_7 conversion for the former reached 88%, compared with only 9% for the latter. The activity for the latter at 300 °C is only comparable with that for the former at 250 °C. However, according to the isomerization thermodynamic equilibrium [3], the lower reaction temperature gives high multibranched isomer selectivity.

To investigate the reason for the significant difference in activity due to the impregnation procedure used, related characterizations were carried out. As shown in Fig. 10, pyridine-FTIR characterization gave Brønsted acid site-to-Lewis acid site ratios of 0.85 and 0.83 for $Pt/WO_3/ZrO_2$ using $Zr(OH)_4$ and ZrO_2 for impregnation, respectively. The only slight difference indicates that acid sites can be created from both impregnation procedures, contrary to findings reported previously [31]. That earlier report claimed that superacid sites are created by impregnation not on the crystallized oxide, but rather on the amorphous form, with subsequent calcination converting it to crystalline form. Fig. 11 displays the crystalline phase difference between these two samples. $Pt/WO_3/ZrO_2$ using $Zr(OH)_4$

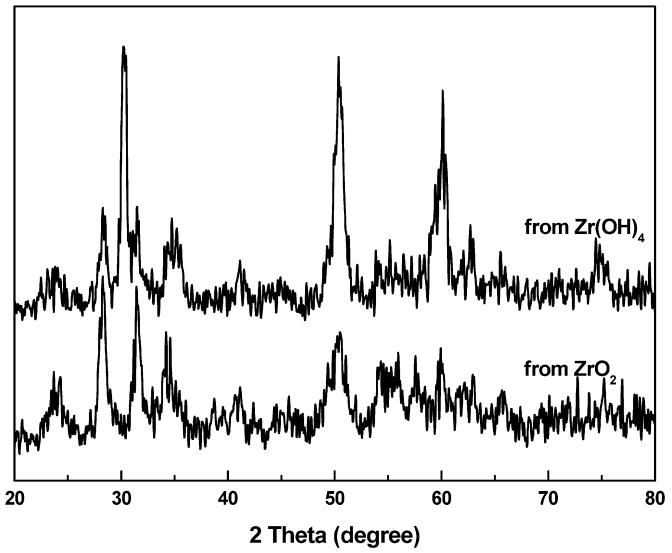

Fig. 11. XRD patterns of $Pt/WO_3/ZrO_2$ impregnated with either $Zr(OH)_4$ or ZrO_2.

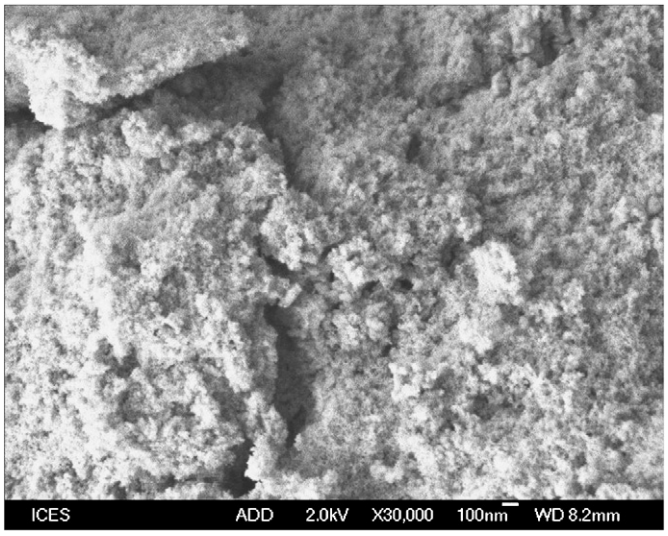

Fig. 12. SEM micrographs of $ZnO–ZrO_2$ after acid treatment.

as the catalyst support is a mixture of tetragonal and monoclinic phases, with tetragonal the dominant phase. However, the catalyst with ZrO_2 as the support is a pure monoclinic phase. As mentioned in Section 3.2, WO_x species homogeneously distributed on the surface of the tetragonal ZrO_2 are the active species for the isomerization reaction [11,12,24]. This may be why the latter showed low activity for n-C_7 hydroisomerization even though their Brønsted acid site-to-Lewis acid site ratios were comparable. Another reason for this finding may be that the surface area for $Pt/WO_3/ZrO_2$ using ZrO_2 for impregnation was only 44 m^2/g, lower than that for the catalyst using $Zr(OH)_4$ as the catalyst support (60 m^2/g). This led to different WO_x surface densities, 11.8 and 8.6 W/nm^2, respectively. It has been reported that WO_x surface density influences the size and electronic properties of WO_x domains and the rate of catalytic reaction [32]. No obvious difference was revealed on XPS analysis.

3.6. Acid treatment for $ZnO–ZrO_2$

As discussed in Sections 3.1 and 3.3, $Pt/WO_3/ZnO–ZrO_2$ with 22 wt% ZnO maintained the tetragonal phase of ZrO_2 but showed no activity for n-C_7 hydroisomerization. Indeed, pyridine-FTIR characterization (Fig. 9) showed the absence of Brønsted acid sites for this catalyst, due to the basic character of ZnO, which neutralized all of the Brønsted acid sites from WO_3/ZrO_2. To recover the Brønsted acid sites, $ZnO–ZrO_2$ was treated by diluted hydrochloride acid. The acid-treated catalysts were then characterized using SEM-EDX, BET, and pyridine FTIR. It is found that the morphology of the surface (Fig. 12) was highly coarse compared with the nontreated catalyst, accompanied by an increase in surface area from 73 to 91 m^2/g. The superficial Zn:Zr ratio dropped to 0.15, much lower than the original Zn:Zr ratio of 0.43. The pyridine-FTIR characterization shown in Fig. 13 indicates that extra Brønsted acid sites were regenerated after acid treatment; these acid sites re-

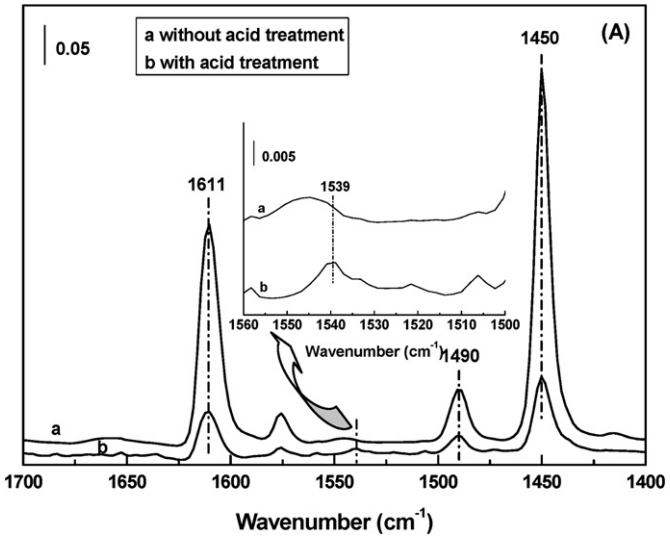

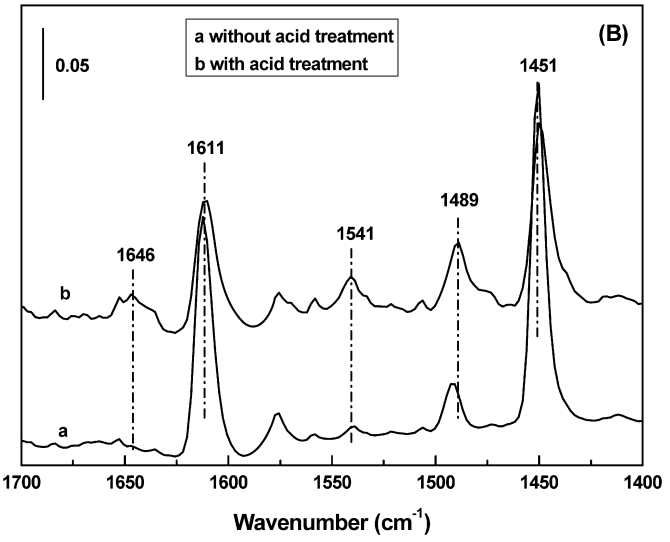

Fig. 13. Pyridine-FTIR characterizations before (A) and after (B) in situ H_2 reduction for $Pt/WO_3/ZnO–ZrO_2$ with and without acid treatment.

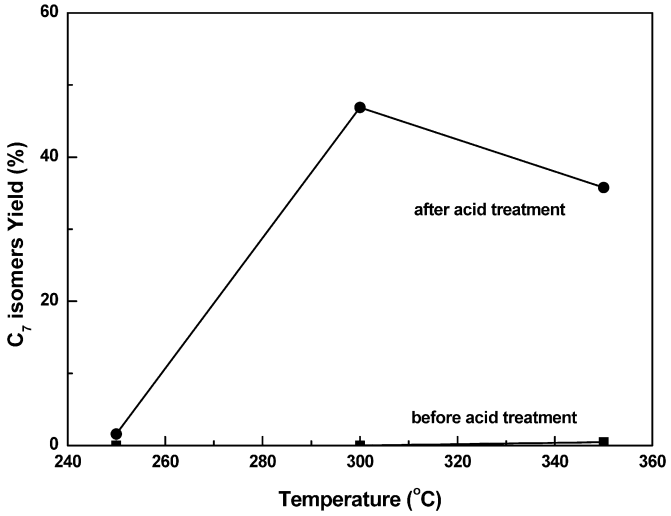

Fig. 14. Acid treatment effects on $Pt/WO_3/ZnO–ZrO_2$ catalytic activity for n-C_7 hydroisomerization (catalyst: 300 mg; Pt: 0.5 wt%; WO_3: 20 wt%; ZnO: 22 wt%; reduction: H_2, 30 ml/min, 400 °C, 2 h; reaction: 300 °C, 0.1 MPa, H_2/n-$C_7 = 30{:}1$).

mained detectable after in situ H_2 reduction. XRD analysis (not shown here) indicated no significant difference between these two samples; both are mixtures of tetragonal and monoclinic phases.

ZnO and ZrO_2 before and after acid treatment were investigated for n-C_7 hydroisomerization after loading of WO_3 and Pt. As shown in Fig. 14, the activity was greatly enhanced at relatively high temperatures, suggesting that the weak and mild acid sites were recovered first. The C_7 isomer yield reached 47% at 300 °C (with conversion and C_7 isomer selectivity of 49% and 96%, respectively). At this temperature, no activity was obtained for the nontreated catalyst $Pt/WO_3/ZnO–ZrO_2$. This suggests that the novel surface properties created after acid activation (e.g., relatively higher surface area and increased number of Brønsted acid sites, lower the surface Zn:Zr ratio) do increase the isomerization activity for $Pt/WO_3/ZnO–ZrO_2$ catalysts. After acid treatment, the activity for $Pt/WO_3/ZnO–ZrO_2$ was comparable even to that for $Pt/WO_3/ZrO_2$ (using ZrO_2 for impregnation; Table 1). Acid treatment had no significant affect on the activity for ZrO_2-supported catalysts.

4. Conclusion

$Pt/WO_3/ZrO_2$ tested with a WO_3 loading optimized at 20 wt% showed good reactivity toward n-heptane hydroisomerization at relatively high temperatures (around 250 °C). Adding ZnO to the catalyst is an alternative approach to achieving the highest C_7 isomer yield (72%) at 250 °C, with a ZnO content of 3.4 wt% in this study. This catalyst exhibited a constant n-heptane hydroisomerization performance for at least 82 h with high n-C_7 conversion (81%) and C_7 isomer selectivity (89%). The reactive crystalline phase is proposed to be the tetragonal phase, which is stabilized by adding WO_3 and ZnO. For the high-ZnO content (22 wt%) $Pt/WO_3/ZnO–ZrO_2$ catalyst, acid treatment at 300 °C greatly improved the C_7 isomer yield, from nil to 47%.

Acknowledgments

Y. Liu thanks Drs. Keith Carpenter and P.K. Wong for their support in this study (project code ICES/02-112001).

References

[1] T.G. Kaufmann, A. Kaldor, G.F. Stuntz, M.C. Kerby, L.L. Ansell, Catal. Today 62 (2000) 77.
[2] I.E. Maxwell, J.E. Naber, Catal. Lett. 12 (1992) 105.
[3] Y. Rezgui, M. Guemini, A. Tighezza, A. Bouchemma, Catal. Lett. 87 (2003) 11.
[4] N. Bouchenafa-Saïb, R. Issaadi, P. Grange, Appl. Catal. A 259 (2004) 9.
[5] T. Okuhara, J. Jpn. Petrol. Inst. 47 (2004) 1.
[6] J.F. Kriz, T.D. Pope, M. Stanciulescu, J. Monnier, Ind. Eng. Chem. Res. 37 (1998) 4560.
[7] T.K. Cheung, B.C. Gates, Chemtech. Sep. (1997) 28.
[8] G.A. Olah, J. Am. Chem. Soc. 94 (1972) 808.
[9] E. Iglesia, S.L. Soled, G.M. Kramer, J. Catal. 144 (1993) 238.
[10] J.G. Santiesteban, D.C. Calabro, W.S. Borghard, C.D. Chang, J.C. Vartuli, Y.P. Tsao, M.A. Natal-Santiago, R.D. Bastian, J. Catal. 183 (1999) 314.
[11] D.G. Barton, S.L. Soled, G.D. Meitzner, G.A. Fuentes, E. Iglesia, J. Catal. 181 (1999) 57.
[12] S. Zhang, Y. Zhang, J.W. Tierney, I. Wender, Appl. Catal. A 193 (2000) 155.
[13] M.A. Arribas, F. Márquez, A. Martínez, J. Catal. 190 (2000) 309.
[14] S. Zhang, Y. Zhang, J.W. Tierney, I. Wender, Fuel Process. Technol. 69 (2001) 59.
[15] P. Pérez-Romo, C. Potvin, J.-M. Manoli, G. Djéga-Mariadassou, J. Catal. 205 (2002) 191.
[16] W. Hua, J. Sommer, Appl. Catal. A 232 (2002) 129.
[17] E. Iglesia, D.G. Barton, S.L. Soled, S. Moseo, J.E. Baumgartner, W.E. Gates, G.A. Fuentes, G.D. Meitzner, Stud. Surf. Sci. Catal. 101 (1996) 533.
[18] E. Iglesia, S.L. Soled, G.M. Kramer, J. Catal. 144 (1993) 238.
[19] E. Blomsma, J.A. Martens, P.A. Jacobs, J. Catal. 159 (1996) 323.
[20] J.W. Ward, Stud. Surf. Sci. Catal. 16 (1983) 587.
[21] I.E. Maxwell, W.H.J. Stork, Stud. Surf. Sci. Catal. 58 (1991) 571.
[22] R.A. Royse, E.I. Ko, J. Catal. 171 (1997) 191.
[23] J.G. Santiesteban, J.C. Vartuli, S. Han, R.D. Bastian, C.D. Chang, J. Catal. 168 (1997) 431.
[24] M.A. Cortés-Jácome, J.A. Toledo, C. Angeles-Chavez, M. Aguilar, J.A. Wang, J. Phys. Chem. B 109 (2005) 22730.
[25] T. Bécue, J.-M. Manoli, C. Potvin, C. Djéga-Mariadassou, J. Catal. 170 (1997) 123.
[26] M.J. Girgis, Y.P. Tsao, Ind. Eng. Chem. Res. 35 (1996) 386.
[27] S. Triwahyono, T. Yamada, H. Hattori, Appl. Catal. A 242 (2003) 101.
[28] S. Triwahyono, T. Yamada, H. Hattori, Appl. Catal. A 250 (2003) 75.
[29] C.A. Emeis, J. Catal. 141 (1993) 347.
[30] Y. Li, W. Zhang, L. Zhang, Q. Yang, Z. Wei, Z. Feng, C. Li, J. Phys. Chem. B 108 (2004) 9739.
[31] K. Arata, M. Hino, Mater. Chem. Phys. 26 (1990) 213.
[32] C.D. Baertsh, S.L. Soled, E. Iglesia, J. Phys. Chem. B 105 (2001) 1320.